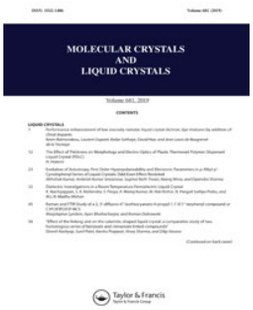

Molecular Crystals and Liquid Crystals

ISSN: 1542-1406 (Print) 1563-5287 (Online) Journal homepage: https://www.tandfonline.com/loi/gmcl20

Intramolecular Charge Transfer Mechanism in Donor-Acceptor Type Triphenylene Meso-substituted Boron-dipyrromethene

Yuefeng Bai, Yang Wang, Jie Cheng, Wentao Yang, Ping Hu & Guanghui Ning

To cite this article: Yuefeng Bai, Yang Wang, Jie Cheng, Wentao Yang, Ping Hu & Guanghui Ning (2019) Intramolecular Charge Transfer Mechanism in Donor-Acceptor Type Triphenylene Meso-substituted Boron-dipyrromethene, Molecular Crystals and Liquid Crystals, 681:1, 77-90, DOI: 10.1080/15421406.2019.1651530

To link to this article: https://doi.org/10.1080/15421406.2019.1651530

Published online: 23 Aug 2019.

MOLECULAR CRYSTALS AND LIQUID CRYSTALS
2019, VOL. 681, NO. 1, 77–90
https://doi.org/10.1080/15421406.2019.1651530

Intramolecular Charge Transfer Mechanism in Donor-Acceptor Type Triphenylene Meso-substituted Boron-dipyrromethene

Yuefeng Bai[a,b], Yang Wang[a], Jie Cheng[b], Wentao Yang[a], Ping Hu[b], and Guanghui Ning[b]

[a]School of Materials Science and Engineering, University of Science & Technology Beijing, Beijing, P. R. China; [b]College of Chemistry and Materials Science, Sichuan Normal University, Chengdu, Sichuan province, P. R. China

ABSTRACT

To investigate the photophysical properties of intramolecular charge transfer mechanism, three boron-dipyrromethene derivatives with different bulk sizes of polyaromatic hydrocarbon at meso-position have been synthesized and fully characterized. The thermodynamics test results revealed that the triphenylene meso-substituted-boron-dipyrromethene possesses the highest thermal stability comparing with the boron-dipyrromethene compounds which meso-position has been substituted by triphenylamine or tetraphenylethylene. The thermal decomposition temperature and melting point of triphenylene meso-substituted-boron-dipyrromethene are up to 369 °C and 297 °C, respectively. The UV-Vis absorption spectra, fluorescence emission spectra and quantum chemical calculations indicated the significant intramolecular charge transfer characteristic from Donor (triphenylene) to Acceptor (BODIPY) moiety.

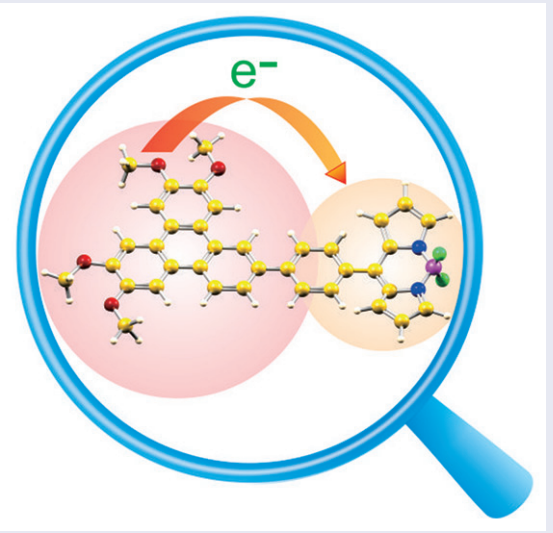

KEYWORDS

Intramolecular charge transfer; Donor-acceptor; Fluorescence; BODIPY; Triphenylene

CONTACT Y. Bai byf610327@163.com; P. Hu hp_x@163.com

Color versions of one or more of the figures in the article can be found online at www.tandfonline.com/gmcl.

Supplemental data for this article can be accessed here.

1. Introduction

Near-infrared (NIR) emitters with visual light as the excitation source are very fascinating in recent years because NIR light can penetrate deeper into most biological tissues and is safety than other visible or ultraviolet light for biological imaging or fluorescent probe [1–4]. The original boron-dipyrromethene (BODIPY, 4,4-difluoro-4-bora-3a,4a-diaza-s-indacene) owns emission at about 500 nm and absorption at the visible region [5]. At the same time, the BODIPY derivatives always present narrow absorption band, high photostability, considerable fluorescence quantum yield and so on [6–9]. Therefore, the illuminant BODIPY has received extensive attention since it was reported by Treibs and Kreuzer in 1968 and various approaches have been presented to obtain NIR-emitting BODIPY derivatives [10–13].

BODIPY always plays a role of strong electron acceptor in the donor-acceptor (D-A) system [14,15]. Generally, the D-A type molecular system possesses a considerable excitation state dipole moment generated by intramolecular charge transfer (ICT) and redistribution of the excited state [16–18]. Therefore, electron can transfer from donor to the fluorophore electron acceptor, and the fluorescence emission can shift to longer wavelength compared to the bare fluorophore. The D-A type molecule simultaneously encompasses good electron accepting properties as well as good hole accepting properties, thus a great deal of efforts have been paid to unearth newly D-A type BODIPY molecule systems and research their exact ICT properties [19–22].

BODIPY structure can be modified at many positions, for instance α-, β-, *meso*-positions and boron-position. A great variety of experimental approaches have been developed to introduce electron donor moieties on BODIPY core to discover the unprecedented function [23–26]. The fluorescence quantum efficient of BODIPY with any substituted group is about 93% in dilute solution of ethanol [27]. As the 3 and 5-position of BODIPY were substituted by methyl and the *meso*-position was substituted by phenyl, the fluorescence quantum efficient of this BODIPY derivative (denote by Phenyl-BODIPY-3,5-DMe) is only 19% in ethanol due to active intramolecular rotations and vibrations [28]. Putting two methyl groups at the 1 and 7-positions of Phenyl-BODIPY-3,5-DMe, and the fluorescence quantum efficiency of this BODIPY derivative (denote as Phenyl-BODIPY-1,3,5,7-TMe) is up to 65% for the reason of stereo-hindrance effect and restriction of the intramolecular rotation. The phenyl group was replaced by pyrene moiety in Phenyl-BODIPY-1,3,5,7-TMe, the fluorescence quantum efficiency of this BODIPY derivative (denote as Pyrene-BODIPY-1,3,5,7-TMe) is about 0.91 in ether [29]. The *p*-position H atom of the benzene cycle in Phenyl-BODIPY-1,3,5,7-TMe was substituted by 9-ethynylanthracene (denote as Anthracene-BODIPY-1,3,5,7-TMe), although the fluorescence quantum efficiency is about 19%, the ICT efficient is over 95% [30]. In 2017, Misra reported a new BODIPY derivative that the meso-position of BODIPY was substituted by phenothiazine and explored the C-T properties in detail [31]. All foregoing studies show that the fluorescence properties of BODIPY can be greatly enhanced according to be substituted with methyl at the α-, β-positions or with larger polyaromatic hydrocarbon (PAH) compounds at the *meso*-position in BODIPY. Triphenylene (TP) is a PAH molecule that fused four benzene cycles together and has been diffusely used in the fields of organic semiconductors

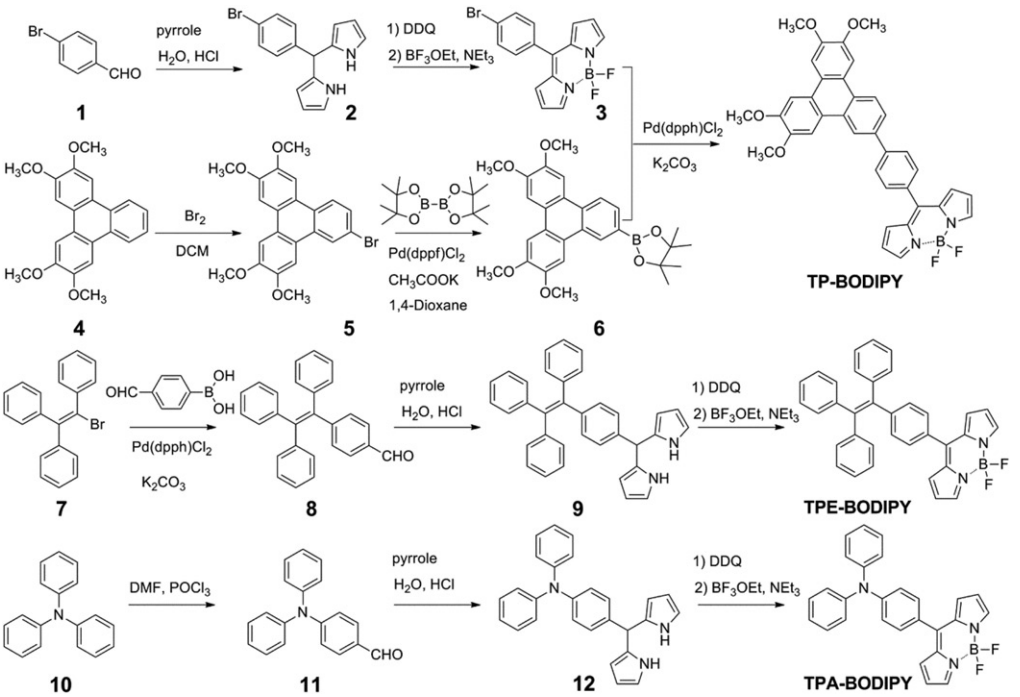

Scheme 1. The synthetic scheme of boron-dipyrromethene derivatives boron-dipyrromethene derivatives with triphenylene (TP-BODIPY), triphenylamine (TPA-BODIPY) or tetraphenylethylene (TPE-BODIPY) molecular fragments as substitution groups at meso-position.

devices such as liquid crystal display, organic light emitting diodes, organic solar cell and so on [32–34].

Herein, to investigate the ICT mechanism in D-A type molecules in detail, we have synthesized a new molecule that the meso-position of BODIPY was substituted by 2,3,6,7-tetramethoxyltriphenylene (TP-BODIPY). The compound TPA-BODIPY which the meso-position of BODIPY was substituted by triphenylamine [35] and TPE-BODIPY which the meso-position of BODIPY was substituted by tetraphenylethylene [36] also have been synthesized to compare and confirm our conclusions. The synthesis procedures are shown in Scheme. 1.

2. Experimental

2.1. Chemicals and instruments

NMR spectrum was recorded at room temperature on Varian 400 MHz spectrometer, using $CDCl_3$ as the solvent and the chemical shifts are given in ppm (δ) relative to tetramethylsilane (TMS). High Resolution Mass (HRMS) was run on Bruker Autoflex III (MALDI-TOF-MS). The thermal properties were studied using differential scanning calorimetry (DSC) and thermal gravimetric analysis (TGA) which were performed on TA Discovery series. UV/Vis absorption spectra were recorded on Perkin Elmer Lambda 950 spectrophotometer. Fluorescence spectra were recorded on HORIBA Fluoromax-4p. Element analysis was carried out on EA 3000.

Pyrrole was purified by distilling under vacuum distillation and other reagents were purchased from commercial suppliers and used as received unless otherwise indicated.

2.2. Synthesis

2.2.1. Br-Phenyl-BODIPY (3)

50 mL 0.12 M hydrochloric acid was added into fresh distil pyrrole (2.2 g, 32.8 mmol) under stirring at room temperature for ten minutes, then 4-bromobenzaldehyde (1.0 g, 5.4 mmol) was dropped into the solution slowly and stirred further 30 minutes. As the reaction finished when detected by TLC, the mixture was washed with D. I. water, and extracted with dichloromethane (DCM, 60 mL*3). The organic layer was dried with anhydrous $MgSO_4$, and DCM was removed by rotavapor, affording crude product **2**.

The crude product **2** was dissolved into 15 mL DCM, and DDQ (1.1 g, 5.0 mmol) was added at N_2 atmosphere, then 3 mL boron fluoride ethyl ether ($BF_3{\cdot}(C_2H_5)_2O$)) and triethylamine were injected into the solution, respectively. After stirring for 5 h, 50 mL H_2O was added to quench the reaction and then extracted with DCM. The organic layer was dried with anhydrous $MgSO_4$, and DCM was removed by rotavapor. The crude product was purified by column chromatography (silica gel, eluting with DCM and PE, V_{DCM}: V_{PE} = 1: 1) further and afford product **3** as an orange crystal by recrystallization from ethanol and ethyl acetate (EA). The total yield is 300 mg, 26%. ^{1}H NMR (400 MHz, $CDCl_3$) δ (ppm): 7.96 (s, α-H, 2 H), 7.69 (d, ArH, J = 8.4 Hz, 2 H), 7.45 (d, ArH, J = 8.8 Hz, 2 H), 6.91 (d, γ-H, J = 4.0 Hz, 2 H), 6.56 (d, β-H, J = 4.0 Hz, 2 H). ^{13}CNMR ($CDCl_3$) δ (ppm): 144.55, 132.57, 131.83, 131.31, 125.51, 118.86, 118.83, 118.81, 118.79. HRMS (MALDI-TOF): calculated for $C_{15}H_{10}BBrF_2N_2$ $[M]^+$, 346.0088; found:346.0084.

2.2.2. TP(OCH$_3$)$_4$ (4)

The intermediates **4** was synthesized according to the report [34] and white solid was obtained with yield 2.5 g, 81%. ^{1}H NMR (400 MHz, $CDCl_3$) δ (ppm): 8.33 - 8.35 (m, ArH, 2 H), 7.76 (s, ArH, 2 H), 7.53 - 7.55 (m, HAr, 2 H), 7.46 (s, ArH, 2 H), 4.03 (s, OCH_3, 6 H), 4.05 (s, OCH_3, 6 H). ^{13}C NMR ($CDCl_3$) δ (ppm): 148.95, 148.41, 128.63, 125.79, 123.56, 123.16, 122.68, 109.99, 104.13, 103.65, 55.85, 55.78. HRMS (MALDI-TOF): calculated for $C_{22}H_{20}O_4$ $[M]^+$, 348.1362; found: 348.1356.

2.2.3. TP(OCH$_3$)$_4$Br (5)

The intermediate compound **4** (1.0 g, 2.87 mmol) was dissolved into 100 mL dry DCM in ice water, then Br_2 (0.69 g, 4.32 mmol) was dissolved into 20 mL DCM, and was droped into the solution slowly among 30 min. The mixture was stirred at room temperature for another 30 min. As the reaction finished which detected by TLC, saturated sodium thiosulfate solution was added until the solution turned into light yellow, and extracted with DCM, dried with anhydrous $MgSO_4$, and concentration. The crude product was purified by column chromatography (silica gel, eluting with DCM and PE, V_{DCM}/V_{PE} = 3/1) further and afford product **5** as white powder by recrystallization from ethanol and EA, 0.95 g, yield 79%. ^{1}H NMR (400 MHz, $CDCl_3$) δ (ppm): 8.31 (s, ArH, 1 H), 8.13 (d, ArH, J = 8.8 Hz, 1 H), 7.69 (s, ArH, 1 H), 7.58 (d, ArH,

$J = 2.0$ Hz, 1 H), 7.53 (d, ArH, $J = 9.2$ Hz, 2 H), 7.47 (s, ArH, 1 H), 4.10 (s, OCH_3, 3 H), 4.08 (s, OCH_3, 3 H), 4.06 (s, OCH_3, 3 H), 4.05 (s, OCH_3, 3 H). ^{13}CNMR ($CDCl_3$) δ (ppm): 149.44, 149.30, 148.63, 148.54, 130.23, 128.55, 127.22, 125.22, 124.39, 123.95, 123.57, 122.56, 121.85, 119.98, 103.98, 103.69, 103.48, 55.95, 55.88. HRMS (MALDI-TOF): calculated for $C_{22}H_{19}BrO_4$ $[M]^+$, 426.0467; found: 426.0461.

2.2.4. TP(OCH_3)$_4$B($OC(CH_3)_2$)$_2$ (6)

A 25 mL round bottle was charged with intermediate **5** (500 mg, 1.1 mmol), bis(pinacolato)diboron (595 mg, 2.3 mmol), 1,1′-bis(diphenylphosphino)ferrocene ($Pd(dppf)_2Cl_2$, 26 mg, 0.03 mmol), potassium acetate (689 mg, 7.0 mmol), 1, 4-dioxane (5 mL) at N_2 atmosphere, and then stirred at 80 °C for 3 h. After the reaction finished, washed with D. I. water, and extracted with DCM. The organic layer was dried with anhydrous $MgSO_4$, and DCM was removed by rotavapor. The crude product was purified by column chromatography (silica gel, eluting with DCM) and obtained product 6 as white powder, 400 mg, yield 72%. ^{1}H NMR (400 MHz, $CDCl_3$) δ (ppm): 8.95 (s, ArH, 1 H), 8.47 (d, ArH, $J = 8.0$ Hz, 1 H), 8.12 (s, ArH, 1 H), 8.0 (d, ArH, $J = 9.2$ Hz, 2 H), 7.78 (s, ArH, 2 H), 4.13 - 4.19 (m, OCH_3, 12 H), 1.44 (s, CH_3, 12 H). ^{13}C NMR ($CDCl_3$) δ (ppm): 149.60, 149.24, 148.75, 148.66, 131.58, 131.00, 129.98, 128.00, 124.44, 123.70, 123.62, 123.22, 121.95, 104.95, 104.74, 103.89, 84.00, 56.27, 55.99, 55.98, 24.96. HRMS (MALDI-TOF): calculated for $C_{28}H_{31}BO_6$ $[M]^+$, 474.2214; found: 474.2207.

2.2.5. TP-BODIPY

The intermediate **3** (49 mg, 0.13 mmol), **6** (30 mg, 0.086 mmol), $Pd(PPh_3)_2Cl_2$ (6.6 mg, 0.01 mmol), potassium carbonate (95.4 mg, 0.69 mmol) were added into 5 mL tetrahydrofuran (THF) and stirred at 70 °C under N_2 atmosphere. After the reaction was finished, 20 mL D. I. water was added, and extracted with DCM. The organic layer was dried with anhydrous $MgSO_4$, and DCM was removed by rotavapor. The crude product was purified by column chromatography (silica gel, eluting with $V_{DCM}/V_{PE} = 2/1$) and obtained the target product **TP-BODIPY** according to recrystallization as red powder, 40 mg, yield 76%. ^{1}H NMR (400 MHz, $CDCl_3$) δ (ppm): 8.71 (s, ArH, 1 H), 8.61 (d, ArH, $J = 8.8$ Hz, 1 H), 8.06 (s, ArH, 1 H), 8.02 (s, ArH, 1 H), 7.98 (s, ArH, 2 H), 7.96 (d, ArH, $J = 8.4$ Hz, 2 H), 7.89 (d, ArH, $J = 8.4$ Hz, 1 H), 7.81 (d, α-H, $J = 8.4$ Hz, 2 H), 7.76 (d, ArH, $J = 8.0$ Hz, 2 H), 7.07 (d, γ-H, $J = 4.4$ Hz, 2 H), 6.59 - 6.60 (m, β-H, 2 H), 4.15 (s, OCH_3, 12 H). ^{13}CNMR ($CDCl_3$) δ (ppm): 149.65, 148.97, 148.94, 147.04, 144.08, 144.03, 137.20, 134.88, 132.79, 131.49, 131.32, 129.17, 128.62, 127.39, 125.04, 124.29, 124.13, 123.79, 123.07, 121.46, 118.60, 104.58, 104.53, 104.19, 104.11, 56.14, 56.08, 56.02, 45.33. Anal. Calcd for ($C_{37}H_{29}BF_2N_2O_4$): C 72.32, H 4.76, N 4.56, found C 72.25, H 4.71, N 4.62. HRMS (MALDI-TOF): calculated for $C_{37}H_{29}BF_2N_2O_4$ $[M + Na]^+$, 637.2086; found: 637.2085.

2.2.6. TPE-BODIPY

Bromotriphenylethylene (500 mg, 1.49 mmol), 4-formylphenylboronic acid (269 mg, 1.97 mmol), bis(triphenylphosphine)palladium(II) chloride, $Pd(PPh_3)_2Cl_2$ (68 mg, 0.09 mmol), potassium carbonate (3.09 mg, 20 mmol) were added into 5 mL THF and

stirred at 70 °C under N_2 atmosphere. After the reaction finished, 20 mL D. I. water was added, and extracted with DCM. The organic layer was dried with anhydrous $MgSO_4$, and DCM was removed by rotavapor. The crude product was purified by column chromatography (silica gel, eluting with V_{DCM}/V_{PE} = 1/4) and obtained product 4-(1,2,2-triphenylvinyl)benzaldehyde **7** as light yellow powder, 450 mg, yield 84%. ^{1}H NMR (400 MHz, $CDCl_3$) δ (ppm): 9.92 (s, CHO 1H), 7.63 (d, ArH, J = 8.4 Hz, 2 H), 7.21 (d, ArH, J = 8.0 Hz, 2 H), 7.13 - 7.15 (m, ArH, 9 H), 7.02 - 7.06 (m, ArH, 6 H).

The precursor **7** (300 mg, 0.83 mmol), fresh distil pyrrol (167.4 mg, 2.50 mmol) were dissolved into 10 mL DCM, and then **2** drops of trifluoroacetic acid was added and stirred at N_2 atmosphere until the start reagent was consumed. DDQ (189 mg, 0.83 mmol) was added into the mixture and further stirred about 30 min, then 2 mL $BF_3{\cdot}(C_2H_5)_2O$ and triethylamine were injected into the solution, respectively, and stirred another 3 h. At the end, 20 mL H_2O was added and quenched the reaction and extracted with DCM. The organic layer was dried with anhydrous $MgSO_4$, and DCM was removed by rotavapor. The crude product was purified by column chromatography (silica gel, eluting with DCM and PE, V_{DCM}: V_{PE} = 1: 1) further and afford product TPE-BODIPY as orange crystal by recrystallization from ethanol and EA. The total yield is 122 mg, 28%. ^{1}H NMR (400 MHz, $CDCl_3$) δ (ppm): 7.92 (s, α-H, 2 H), 7.31 (d, ArH, J = 8.0 Hz, 2 H), 7.04 - 7.19 (m, ArH, 17 H), 6.86 (d, γ-H, J = 4 Hz, 2 H), 6.54 (d, β-H, J = 4 Hz, 2 H). ^{13}CNMR ($CDCl_3$) δ (ppm): 146.89, 143.76, 143.24, 143.02, 142.87, 142.69, 139.73, 134.75, 131.74, 131.35, 131.30, 131.22, 130.04, 127.92, 127.76, 127.73, 126.96, 126.84, 118.37, 118.36. Anal. Calcd for ($C_{35}H_{25}BF_2N_2$): C 80.47, H 4.82, N 5.36, found: C 80.49, H 4.86, N 5.43. HRMS (MALDI-TOF): calculated for $C_{35}H_{25}BF_2N_2$ $[M]^+$, 522.2079; found: 522.2073.

2.2.7. TPA-BODIPY

The synthesis procedure of TPA-BODIPY is same with TPE-BODIPY. 4-(diphenylamino)benzaldehyde (200 mg, 0.74 mmol), pyrrol (98.5 mg, 1.47 mmol), trifluoroacetic acid (2 drops), DDQ (176 mg, 0.74 mmol), $BF_3{\cdot}(C_2H_5)_2O$, 2 mL and trimethylamine (2 mL). Organic crystal and the total yield are 102 mg, 32%. ^{1}H NMR (400 MHz, $CDCl_3$) δ (ppm): 7.90 (s, α-H, 2 H), 7.46 (d, ArH, J = 8.4 Hz, 2 H), 7.36 (t, ArH, J = 7.2 Hz, 4 H), 7.22 (d, ArH, J = 8.0 Hz, 4 H), 7.17 (t, ArH, J = 7.4 Hz, 2 H), 7.10 (d, ArH, J = 8.4 Hz, 2 H), 7.06 (d, γ-H, J = 4.0 Hz, 2 H), 6.55 (t, β-H, J = 4.0 Hz, 2 H). ^{13}CNMR ($CDCl_3$) δ (ppm): 150.94, 146.46, 142.77, 134.59, 134.58, 132.29, 131.06, 129.69, 126.19, 125.96, 124.73, 120.01, 118.01, 117.99, 117.98. Anal. Calcd for ($C_{27}H_{20}BF_2N_3$): C 74.50, H 4.63, N 9.65 found: C 74.34, H 4.65, N 9.70. HRMS (MALDI-TOF): calculated for $C_{27}H_{20}BF_2N_3$ $[M]^+$, 435.1718; found: 435.1712.

3. Results and discussion

3.1. Synthesis and characterization

As depicted in scheme 1, the BODOPY segments were synthesized according to the standard method by using different aldehydes precursors and pyrrole as starting

materials with hydrochloric acid as catalyst. Different aldehydes precursors were obtained from different initial reagents. The TP-BODIPY was synthesized according to join tetramethoxyltriphenylene boric acid ester **6** and *p*-bromobenzene-BODIPY **3** together by Suzuki reaction. *p*-Bromobenzene-BODIPY **3** was converted from *p*-bromobenzaldehyde **1**. TPE-BODIPY was prepared from aldehydes precursors **8** which was synthesized from bromotriphenylethene 7 and (4-formylphenyl)boronic acid by Suzuki reaction too, and this method can obtain single aldehyde group substituted TPE in quantitive easily. TPA-BODIPY was synthesized from 4-(diphenylamino)benzaldehyde **11** and the aldehyde derivative was prepared from TPA **10** in site by Vilsmeier-Haack reaction. All the BODIPY intermediates **2**, **9**, **12** are unstable compounds, and they were oxidized by DDQ and did not isolate further. The structure and purity of final products TP-BODIPY, TPA-BODIPY and TPE-BODIPY were fully characterized by NMR, HRMS and Elemental Analysis.

TPA-BODIPY and TPE-BODIPY which suitable crystal compounds were characterized by single crystal X-ray diffraction further and they are shown in Figure S1. The structural investigation reveals that the two pyrrole cycles in BODIPY part are lie to the same flat surface as for the anchor effect of boron atom. The BODIPY moiety and near benzene cycle in donor moiety in all three product molecules exhibit a large dihedral angle through the single bond rotation and stereo-hindrance effect. Single crystal data shows that the dihedral angles in compound TPA-BODIPY and TPE-BODIPY are 51.5° and 44.6°, respectively.

3.2. Thermal properties

The thermal properties of TP-BODIPY, TPA-BODIPY and TPE-BODIPY were investigated by TGA and DSC as shown in Figures 1, 2 and Table 1. The thermal decomposition temperature (T_d corresponds to the temperature at 5 wt% lost) of TPA-BODIPY

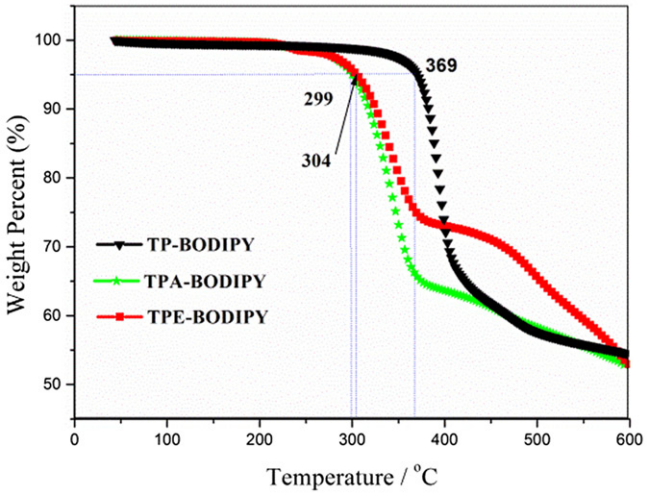

Figure 1. Thermal gravimetric analysis curves of the boron-dipyrromethene derivatives with triphenylene (TP-BODIPY), triphenylamine (TPA-BODIPY) or tetraphenylethylene (TPE-BODIPY) molecular fragments as substitution groups at meso-position.

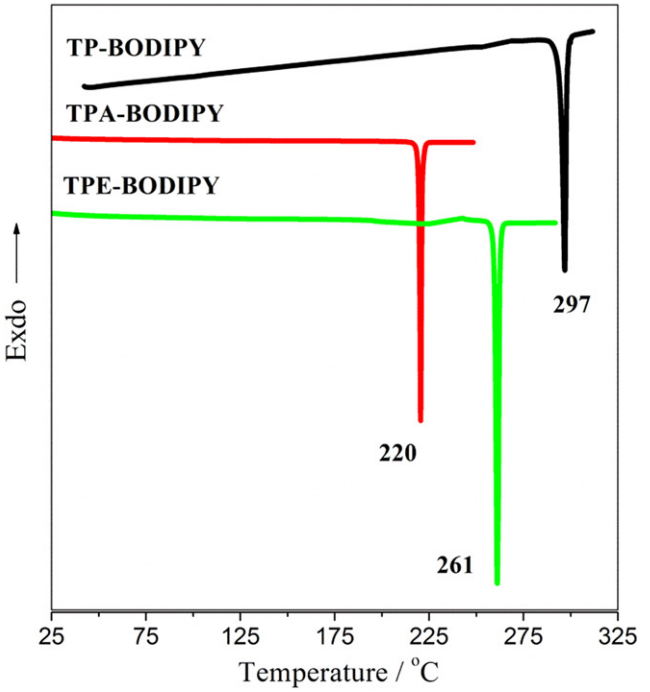

Figure 2. Differential scanning calorimetry curves of the boron-dipyrromethene derivatives with triphenylene (TP-BODIPY), triphenylamine (TPA-BODIPY) or tetraphenylethylene (TPE-BODIPY) molecular fragments as substitution groups at meso-position.

Table 1. Thermal and optical properties of the boron-dipyrromethene derivatives with triphenylene (TP-BODIPY), triphenylamine (TPA-BODIPY) or tetraphenylethylene (TPE-BODIPY) molecular fragments as substitution groups at meso-position

Compd.	T_d / °C	M_p / °C	λ_{abs} / nm	λ_{em} [DCM] / nm	λ_{em} [THF] / nm
TP- BODIPY	369	297	284, 502	654, 718	654, 718
TPA-BODIPY	299	220	300, 498	–	–
TPE- BODIPY	304	261	316, 502	674	634

Note. T_d thermal decomposition temperature (the temperature at 5 wt% lost); Mp melting point; λ_{abs} and λ_{em} were acquired in dilute solution of DCM or THF at the concentration of $1*10^{-6}$ mol/L.

and TPE-BODIPY are 299 °C and 304 °C, respectively. The T_d of TP-BODIPY is much higher than the other two compounds over 70 centigrade and up to 369 °C, which can be attributed to the large π-conjugated system and highly ordered degree in TP-BODIPY. As shown in DSC curves, the compounds TP-BODIPY, TPA-BODIPY and TPE-BODIPY displayed only one narrow melting peak during heating process, the melting temperature are up to 297 °C, 220 °C and 261 °C, respectively. TP-BODIPY also enjoys the highest melting point among the three compounds.

3.3. Photophysical properties

For the purpose of investigating the ICT, the UV-Vis absorption and emission spectra of TP-BODIPY, TPA-BODIPY and TPE-BODIPY were obtained in dilute solution of

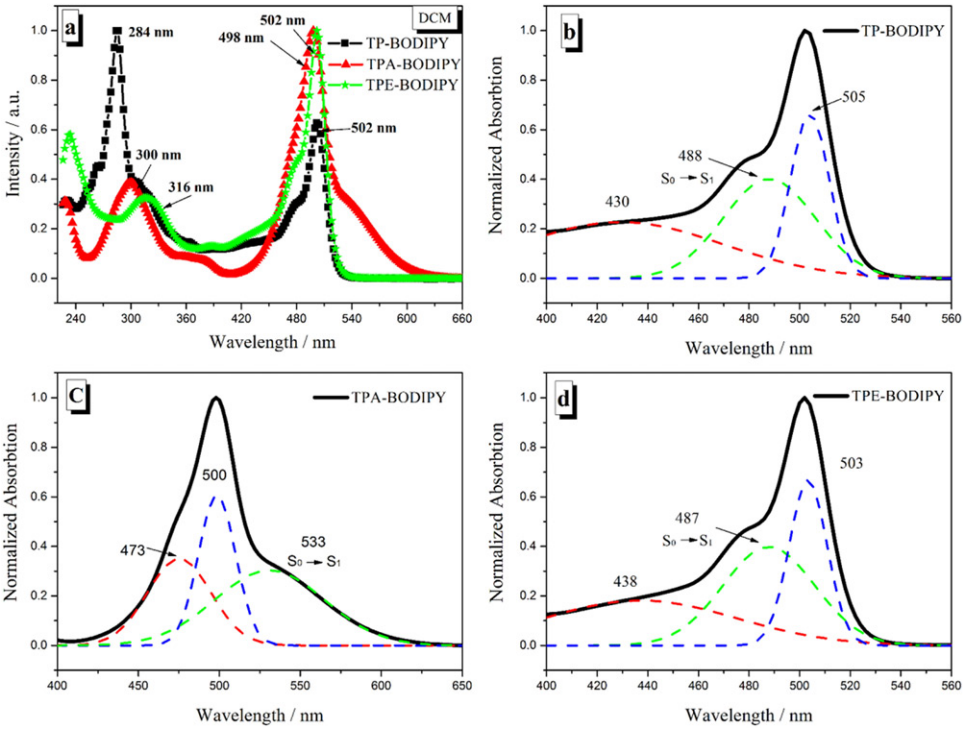

Figure 3. Absorption spectra for the boron-dipyrromethene derivatives with triphenylene (TP-BODIPY), triphenylamine (TPA-BODIPY) or tetraphenylethylene (TPE-BODIPY) as substitution groups at meso-position in dichloromethane (a) and the corresponding deconvolution Guassian bands (b, c, d).

DCM or THF at the concentration of $1*10^{-6}$ mol/L, as shown in Figures 3, 4, S3 and Table 1. In addition, the UV-Vis absorption spectra in ethanol and cyclohexane solvents were also obtained and shown in Figure S2. All the three products exhibited almost the same absorption spectra, and there were about two absorption bands at 220 - 400 nm and 420 - 650 nm in Figure 3a. The maximum absorption peak was located at about 500 nm from 420 to 650 nm, which can be attributed to the absorption peak of BODIPY moiety [37]. TP-BODIPY and TPE-BODIPY represented a shoulder on the high-energy side whereas the shoulder peak of TPA-BODIPY situated at the long wavelength region. The results indicate that the shoulder peaks are the ICT absorption [38]. There are also some peaks in the range of 220 - 400 nm which can be attributed to the absorption of donor moieties in every product molecule. Because of the triphenylene molecule moiety contains larger π-conjugate area than other molecules, the absorption peak at ~284 nm is the strongest among the three compounds and even stronger than the BODIPY moiety absorption peak in TP-BODIPY.

Deconvolution of the absorption spectra in the range of 420 - 650 nm to a series of Gaussian bands for all three compounds are shown in Figure 3b, 3c, 3d. The C-T absorption peaks that centre at ~ 488 nm in TP-BODIPY and TPE-BODIPY are associated with the $S_0 \rightarrow S_1$ electron transition. Owing to the presence of a lone pair electron at the N-atom in TPA-BODIPY, the energy barrier of $S_0 \rightarrow S_1$ electronic transition in TPA-BODIPY is lower than other two compounds and the C-T absorption peak is about 533 nm.

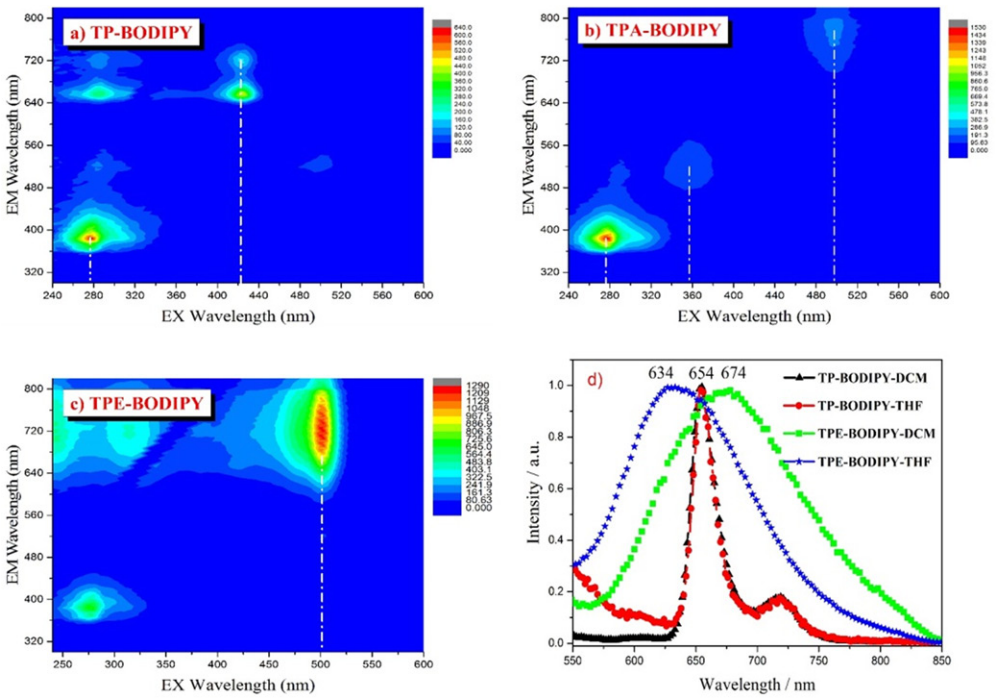

Figure 4. Three-dimensional fluorescence spectra of the boron-dipyrromethene derivatives with triphenylene (a), triphenylamine (b) or tetraphenylethylene (c) as substitution groups at meso-position. (d) One-dimensional fluorescence spectra of triphenylene meso-substituted boron-dipyrromethene (TP-BODIPY) and tetraphenylethylene meso-substituted boron-dipyrromethene (TPE-BODIPY) in different solvents.

Figure 4a, 4b and 4c depict the three-dimensional fluorescence spectra of compounds TP-BODIPY, TPA-BODIPY and TPE-BODIPY in DCM solvent, respectively. Figure 4d is the one-dimensional fluorescence spectra of compounds TP-BODIPY, TPE-BODIPY in different polarity solvents (THF and DCM).

As shown in Figure 4a, the emission wavelength covers from 360 to 440 nm upon the excitation wavelength of 278 nm, which is corresponding to the local exited (LE) emission of triphenylene moiety in TP-BODIPY. The molecule TP-BODIPY undergoes the ICT upon the light excitation wavelength at about 420 nm, thus the strong red-shift is presented compare to the original BODIPY molecular and eventually the fluorescence emission wavelength in the range of 640 - 730 nm. The emission peak of TP-BODIPY ($\sim$ 654 nm), as shown in Figure 4d, remains stable when the polarity of the solvent changes, and the shoulder peak could be explained by the ICT characteristic.

Figure 4b exhibits a strong emission band at 350 - 440 nm and two much weaker emission bands at longer wavelength region, which can be confirmed by one dimensional fluorescence spectra further at different excitation wavelength (ca. 277 nm, 363 nm and 500 nm) in DCM as shown in Figure S3. The results revealed that the fluorescence intensity of TPA-BODIPY was gradually decreased as the excitation wavelength increased. Therefore, the compound TPA-BODIPY manifested non-emission practically in visual light range when it was dissolved in solvents for the active intramolecular rotations and vibrations. It is clear shown that the strongest emission band of compound TPE-BODIPY is around 620 - 820 nm upon

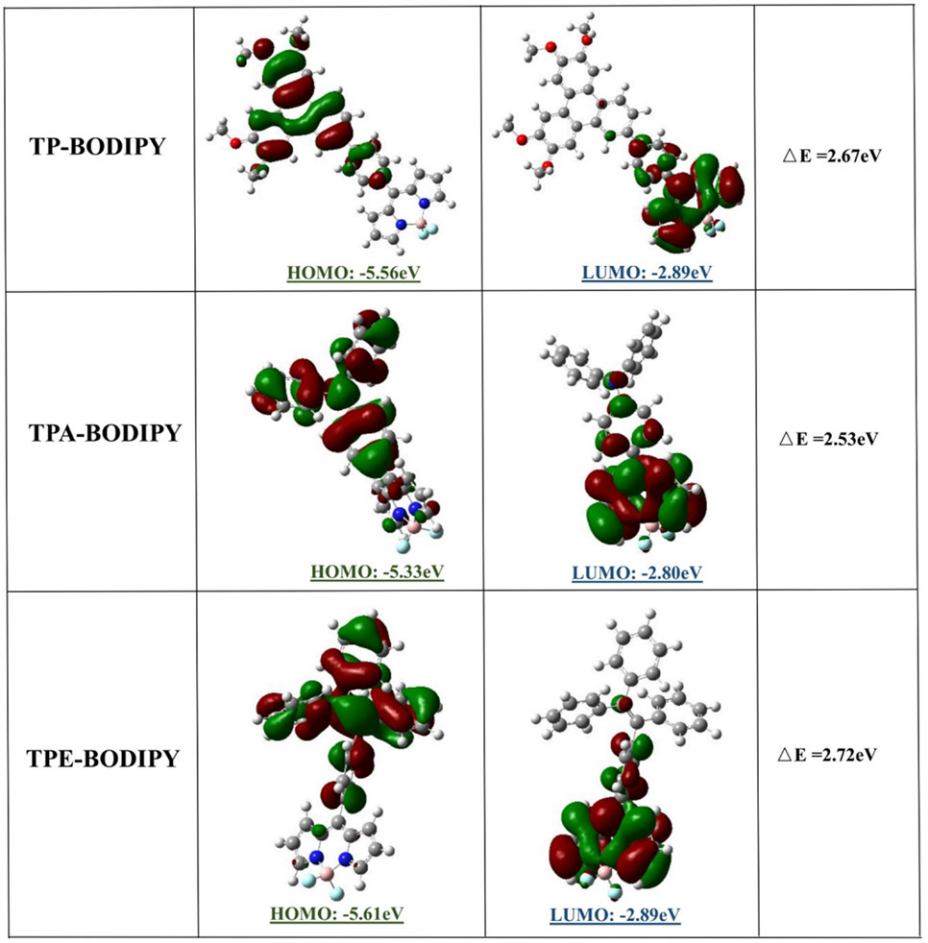

Figure 5. Energy-minimized structure (B3LYP/6-31G(d,p)/PCM (dichloromethane) of boron-dipyrromethene derivatives with triphenylene (TP-BODIPY), triphenylamine (TPA-BODIPY) or tetraphenylethylene (TPE-BODIPY) as substitution groups at meso-position.

the excitation wavelength 500 nm in Figure 4c. The fluorescence emission results of TPA-BODIPY and TPE-BODIPY are consistent with the previous report, and show the characteristic of Aggregation-induced emission (AIE) effect [35,36]. The emission band at long wavelength is regarded as TICT emission peaks. The emission wavelength of TPE-BODIPY presents a red-shift from 634 nm to 674 nm as the solvent changed from THF to DCM, namely the TPE-BODIPY possesses conspicuous solvatochromic properties and large red-shift as the solvent polarity increased.

3.4. Quantum chemical calculations

The interaction between electron donor and acceptor moieties in compounds TP-BODIPY, TPA-BODIPY and TPE-BODIPY was investigated through quantum chemical calculations with the software package of Gaussian 09 [39]. Density functional theory (DFT) and time-dependent DFT (TD-DFT) were performed at B3LYP/6-31G (d, p) level. The excitation

Table 2. Computed excitation energies, oscillator strengths, and dominant transitions for the boron-dipyrromethene derivatives with triphenylene (TP-BODIPY), triphenylamine (TPA-BODIPY) or tetraphenylethylene (TPE-BODIPY) molecular fragments as substitution groups at meso-position

Compd.	Excite state	Main transition(coefficient)	Main character	Excitation energy (eV)	λ / nm	f	$\lambda^{calcd.}$ / nm
TP- BODIPY	S_1	HOMO → LUMO (0.700)	$\pi_{TP} \rightarrow \pi^*_{BODIPY}$, ICT	2.36	526	0.222	505
	S_3	HOMO-2 → LUMO (0.684)	$\pi_{BODIPY} \rightarrow \pi^*_{BODIPY}$, LE	2.95	419	0.407	
TPA-BODIPY	S_1	HOMO → LUMO (0.706)	$\pi_{TPA} \rightarrow \pi^*_{BODIPY}$, ICT	2.13	583	0.335	498
	S_2	HOMO-1 → LUMO (0.686)	$\pi_{BODIPY} \rightarrow \pi^*_{BODIPY}$, LE	2.98	416	0.415	
TPE- BODIPY	S_1	HOMO → LUMO (0.705)	$\pi_{TPE} \rightarrow \pi^*_{BODIPY}$, ICT	2.32	535	0.195	502
	S_2	HOMO-1 → LUMO (0.684)	$\pi_{BODIPY} \rightarrow \pi^*_{BODIPY}$, LE	2.96	419	0.405	

energies, main characters and oscillator strengths have been calculated with the optimized configuration of the polarizable continuum model (PCM) in DCM.

The frontier orbital plots of the highest occupied molecular orbital (HOMO) and lowest unoccupied molecular orbital (LUMO) are shown in Figure 5. The LUMO levels of all three compounds are mainly localized on the BODIPY moiety and the HOMO levels are mainly localized on the TP, TPA and TPE moieties respectively, which clearly shows that the strong ICT behaviour from donors TP, TPA or TPE to accepter BODIPY moiety in TP-BODIPY, TPA-BODIPY and TPE-BODIPY as previous reports [40]. The theoretical calculated HOMO energies of TP-BODIPY, TPA-BODIPY and TPE-BODIPY are −5.56 eV, −5.33 eV and −5.61 eV respectively and the corresponding LUMO energies are −2.89 eV, −2.80 eV and −2.89 eV respectively. Therefore, the electron donating ability is TPA > TP > TPE. The energy gap between HOMO and LUMO of TP-BODIPY, TPA-BODIPY and TPE-BODIPY are 2.67 eV, 2.53 eV and 2.72 eV respectively and follow the order of TPE-BODIPY > TP-BODIPY > TPA-BODIPY. According to calculation, the dihedral angles between BODIPY moiety and the adjacent benzene cycle in donor moiety are 51°, 48° and 52° in corresponding to TP-BODIPY, TPA-BODIPY and TPE-BODIPY.

The excite states, mainly transitions, excitation energies and oscillator strengths were obtained from TD-DFT calculation and listed in Table 2. The first 10 excited transitions results indicate that there are two main electronic transitions in the visible region for all the three D-A type BODIPY compounds. The excited state with the most powerful oscillator strength in every compound occurs at the local excitation of BODIPY moiety in the visible region and respectively corresponding to the transitions of HOMO-2 → LUMO in TP-BODIPY, HOMO-1 → LUMO in TPA-BODIPY and TPE-BODIPY. The relevant molecular orbital maps are listed in Figure S4. The excited state with the secondary strong oscillator is the HOMO → LUMO transition among in three compounds and it is associated with the TICT characteristic from the TP, TPA or TPE moiety to BODIPY moiety. The theoretical calculation results agree qualitatively with the experimental UV-vis values and the results of the deconvolution absorption spectrum in visible region as described before.

4. Conclusion

Three D-A type meso-substituent BODIPY derivative TP-BODIPY, TPA-BODIPY and TPE-BODIPY have been smoothly synthesized and fully characterized by NMR, HRMS

and Element analysis. Compared with the meso-substituents BODIPY derivatives by units TPA and TPE, the TP-BODIPY displays the highest thermal decomposition temperature and melting point, and up to 369 °C and 297 °C, respectively. All the three products exhibit almost the same absorption spectrums in different solvents such as ethanol, DCM, THF and hexane. The absorption band at 420–650 nm can be attributed to the absorption of BODIPY moiety, while the absorption band at 220–400 nm can be attributed to the absorption of donor moieties in every product molecule. Deconvolution of the absorption spectrums in the range of 420–650 nm indicate that the C-T absorption peaks, which centred at ∼488 nm in TP-BODIPY and TPE-BODIPY, are associated with the $S_0 \rightarrow S_1$ electronic transition and the energy barrier of $S_0 \rightarrow S_1$ electronic transition in TPA-BODIPY is lower than other two compounds at 533 nm. Because of the ICT, the fluorescence emission of TP-BODIPY red shift from 500 to 654 nm compared with the original BODIPY molecular, and the shoulder peak can be attributed to ICT emission. The theoretical calculation results show a qualitative agreement with the experimental UV-vis values and the results of the deconvolution absorption spectrum in visible region. The LUMO levels of all three compounds are mainly localized on the BODIPY moiety and the HOMO levels are mainly localized on the TP, TPA or TPE moieties, respectively. It suggests that there is strong ICT effect from the electron donor TP, TPA or TPE to acceptor BODIPY moiety in TP-BODIPY, TPA-BODIPY and TPE-BODIPY respectively.

Acknowledgements

This work was supported by the National Natural Science Foundation of China under Grant [51073112, 51443004]; The Youth Foundation of Sichuan Educational Committee under Grant [18ZB0497]; and Foundation for Research and Development in Experiment Technic of Sichuan Normal University under Grant [SYJS2017008].

References

[1] Iwano, S., Sugiyama, M., Hama, H., Watakabe, A., Hasegawa, N., Kuchimaru, T., Tanaka, K. Z., Takahashi, M., Ishida, Y., Hata, J., Shimozono, S., Namiki, K., Fukano, T., Kiyama, M., Okano, H., Kizaka-Kondoh, S., McHugh, T. J., Yamamori, T., Hioki, H., Maki, S., & Miyawaki, A. (2018). *Science*, *359*, 935–939.
[2] Barnes, R. B. (1963). *Science*, *140*, 870–877.
[3] Yue, X., Zhang, Q., & Dai, Z. (2017). *Adv. Drug Deliver. Rev.*, *115*, 155–170.
[4] Asano, T., Suemitsu, M., Hashimoto, K., Zoysa, M. D., Shibahara, T., Tsutsumi, T., & Noda, S. (2016). *Sci. Adv.*, *2*, e1600499.
[5] Loudet, A., & Burgess, K. (2007). *Chem. Rev.*, *107*, 4891–4932.
[6] Pascal, S., Bucher, L., Desbois, N., Bucher, C., Andraud, C., & Gros, C. P. (2016). *Chem. Eur. J.*, *22*, 4971–4979.
[7] Ulrich, G., Ziessel, R., & Harriman, A. (2008). *Angew. Chem. Int. Ed.*, *47*, 1184–1201.
[8] Wei, X., Bu, L., Li, X., Ågren, H., & Xie, Y. (2017). *Dyes Pigments*, *136*, 480–487.
[9] Er, J. C., Tang, M. K., Chia, C. G., Liew, H., Vendrell, M., & Chang, Y. T. (2013). *Chem. Sci.*, *4*, 2168–2176.
[10] Treibs, A., & Kreuzer, F. (1968). *Justus Liebigs Ann. Chem.*, *718*, 208–223.
[11] Boens, N., Leen, V., & Dehaen, W. (2012). *Chem. Soc. Rev.*, *41*, 1130–1172.
[12] Lu, H., Mack, J., Yang, Y., & Shen, Z. (2014). *Chem. Soc. Rev.*, *43*, 4778–4823.

[13] Hiruta, Y., Koiso, H., Ozawa, H., Sato, H., Hamada, K., Yabushita, S., Citterio, D., & Suzuki, K. (2015). *Org. Lett.*, *17*, 3022–3025.
[14] Popere, B. C., Pelle, A. M. D., & Thayumanavan, S. (2011). *Macromolecules*, *44*, 4767–4776.
[15] Hinton, D.A., Ng, J.D., Sun, J., Lee, S., Saikin, S. K., Logsdon, J., White, D.S., Marquard, A.N., Cavell, A.C., Krasecki, V.K., Knapper, K.A., Lupo, K.M., Wasielewski, M.R., Aspuru-Guzik, A., Biteen, J.S., Gopalan, P., & Goldsmith, R.H. (2018). J. Am. Chem. Soc., 140, 15827–15841.
[16] Li, Z., Liu, W., Yu, Y., Lv, X., Si, C., Wu, Z., Cui, Y., Jia, H., Yu, J., Wang, H., Shi, F., & Hao, Y. (2015). *Dyes Pigments*, *122*, 238–245.
[17] Thakare, S. S., Chakraborty, G., More, A. B., Chattopadhyay, S., Mula, S., Ray, A. K., & Sekar, N. (2018). *J. Lumin.*, *194*, 622–630.
[18] Li, X., Sun, S., Kim, I. J., & Son, Y. A. (2017). *Mol. Cryst. Liq. Cryst.*, *654*, 139–145.
[19] Heyer, E., & Ziessel, R. (2013). *Tetrahedron Lett.*, *54*, 3388–3393.
[20] Lee, S. N., Lee, S. J., Kim, Y. K., & Shin, D. M. (2013). *Mol. Cryst. Liq. Cryst.*, *581*, 59–69.
[21] Zhang, X., Zhang, Y., Chen, L., & Xiao, Y. (2015). *RSC Adv.*, *5*, 32283–32289.
[22] Bozdemir, O. A., Cakmak, Y., Sozmen, F., Ozdemir, T., Siemiarczuk, A., & Akkaya, E. U. (2010). *Chem. Eur. J.*, *16*, 6346–6351.
[23] Dhokale, B., Gautam, P., Mobina, S. M., & Misra, R. (2013). *Dalton Trans.*, *42*, 1512–1518.
[24] Kurowska, A., Brzeczek-Szafran, A., Zassowski, P., Lapkowski, M., Domagala, W., Wagner, P., & Wagner, K. (2018). *Electrochim Acta.*, *271*, 685–698.
[25] Chapran, M., Angioni, E., Findlay, N. J., Breig, B., Cherpak, V., Stakhira, P., Tuttle, T., Volyniuk, D., Grazulevicius, J. V., Nastishin, Y. A., Lavrentovich, O. D., & Skabara, P. J. (2017). *ACS Appl. Mater. Inter.*, *9*, 4750–4757.
[26] Karmakar, A., Chaudhuri, T., Mula, S., & Chattopadhyay, S. (2015). *Spectrochim Acta. A*, *137*, 1258–1264.
[27] Arroyo, I. J., Hu, R., Merino, G., Tang, B. Z., & Peña-Cabrera, E. (2009). *J. Org. Chem.*, *74*, 5719–5722.
[28] Qin, W., Baruah, M., Auweraer, M. V. der, Schryver, F. C. De, & Boens, N. (2005), *J. Phys. Chem. A*, *109*, 7371–7384.
[29] Yang, Y., Zhang, L., Gao, C., Xu, L., Bai, S., & Liu, X. (2014). *RSC Adv.*, *4*, 38119–38123.
[30] Wan, C. W., Burghart, A., Chen, J., Bergström, F., Johansson, L. B. Å., Wolford, M. F., Kim, T. G., Topp, M. R., Hochstrasser, R. M., & Burgess, K. (2003). *Chem. Eur. J.*, *9*, 4430–4441.
[31] Poddar, M., Gautam, P., Rout, Y., & Misra, R. (2017). *Dyes Pigments.*, *146*, 368–373.
[32] Bai, Y. F., Zhao, K. Q., Hu, P., Wang, B. Q., & Shimizu, Y. (2009). *Mol. Cryst. Liq. Cryst.*, *509*, 60–76.
[33] Szydłowska, J., Sitkiewicz, A., Nazaruk, E., Pociecha, D., Krzyczkowska, P., Krówczyński, A., & Gorecka, E. (2018). *Soft Matter.*, *14*, 2104–2111.
[34] Zhang, K., Bai, Y., Feng, C., Ning, G., Ni, H., Yu, W., Zhao, K., Wang, B., & Hu, P. (2018). *New J. Chem.*, *42*, 272–280.
[35] Hu, R., Lager, E., Aguilar-Aguilar, A., Liu, J., Lam, J. W. Y., Sung, H. H. Y., Williams, I. D., Zhong, Y., Wong, K. S., Peña-Cabrera, E., & Tang, B. Z., (2009). *J. Phys. Chem. C.*, *113*, 15845–15853.
[36] Zhao, Y., He, S., Yang, J., Sun, H., Shen, X., Han, X., & Ni, Z. (2018). *Opt. Mater.*, *81*, 102–108.
[37] Misra, R., Dhokale, B., Jadhav, T., & Mobin, S. M. (2013). *Dalton Trans.*, *42*, 13658–13666.
[38] Derin, Y., Yılmaz, R. F., Baydilek, İ. H., Atalay, V. E., Özdemira, A., & Tutar, A. (2018). *Inorg. Chim. Acta.*, *482*, 130–135.
[39] Frisch, M. J., Trucks, G. W., Schlegel, H. B., Scuseria, G. E., Robb, M. A., Cheeseman, J. R., Scalmani, G., Barone, V., Mennucci, B., & Petersson, G. A. et al., Gaussian 09, Revision A02, Gaussian, Inc., Wallingford, CT, 2009.
[40] Li, Z.; Chen, Y.; Lv, X.; & Fu, W., (2013). *New J. Chem.*, *37*, 3755–3761.